ADSORPTION STUDY OF METAL IONS USING ZIRCONIA NANOPOWDERS

A THESIS SUBMITTED IN PARTIAL FULFILLMENT

OF THE REQUIREMENTS FOR THE DEGREE OF

Bachelor of Technology

in

Ceramic Engineering

By

Sourav Mondal

Under the Guidance of

Prof. Bibhuti B. Nayak

Department of Ceramic Engineering
National Institute of Technology
Rourkela 769008 Odisha

Department of Ceramic Engineering

National Institute of Technology

Rourekla

CERTIFICATE

This is to certify that the thesis entitled "ADSORPTION STUDY OF METAL IONS USING ZIRCONIA NANOPOWDERS" submitted by Mr. Sourav Mondal bearing the roll no. 111CR0103 in partial fulfillment of the requirements for the award of the Bachelor of Technology in Ceramic Engineering at National Institute of Technology, Rourkela is an authentic work carried out by him under my supervision and guidance.

To the best of knowledge, the matter embodied in the thesis has not been submitted to any other university/institute for the award of any degree or diploma.

Place: Rourkela

Date: 26/06/2015

Prof. Bibhuti Bhusan Nayak

Department of Ceramic Engineering

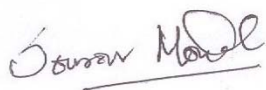National Institute of Technology

Rourkela

Acknowledgement

Table of Contents

Abstract

The present work deals with the synthesis of nanostructured ZrO_2 particles, with and without surfactant (CTAB) for the adsorption of metal ions of Fe (III), Co (II) and Ni (II). The work involves systematic study and analysis of the prepared sample as well as study of the adsorption properties of the prepared sample using various characterization techniques like XRD, BET, UV-Vis spectroscopy and FESEM.

XRD confirmed the phase of the samples as t-ZrO_2 with a crystallite size of 7.3 nm. BET measurements determined the surface area as 55 m^2 g^{-1} with particle size of 19.2 nm. UV-Vis spectroscopy helped in the determination of adsorption isotherm and order of the reaction. Generally the samples followed Freundlich adsorption isotherm and pseudo-second order kinetics.

Fe (III) case showed the highest adsorption among all the three whereas Ni (II) showed lowest adsorption in case of without surfactant and Co (II) showed lowest adsorption in case of with surfactant. Samples with surfactant showed better adsorption phenomenon than samples without surfactant.

Keywords: ZrO_2, surfactant, CTAB, adsorption, BET, XRD, UV-Vis spectroscopy, FESEM

Introduction

The intrinsic physical and chemical properties of ZrO_2 have attracted researchers and scientist over a long span of time. Some of these properties include good wear resistance properties, hardness, elastic modulus, low coefficient of friction, chemical inertness, ionic conductivity, low thermal conductivity, high melting point (2700 °C) and electrical properties. All these properties made ZrO_2 as one of the ideal material for refractory. After the first reporting of transformation toughening in ZrO_2 by Garvie, Hannink and Pascoe [1] in the paper "Ceramic Steel?", ZrO_2 became a research subject for many researchers.

Till date, ZrO_2 ceramics have exhibited the fact that they are the toughest and strongest (single - phase) oxide ceramics produced. ZrO_2 toughened ceramics, toughened by transformation toughening, has been used in many examples. Because of good physical properties like high flexural strength, good fracture toughness and high temperature stability, ZrO_2 is widely used in industrial applications. Recent trends of research and development have focused ZrO_2 in advanced applications like catalyst, biomaterials [2] for dentistry and hip-prosthesis parts, high temperature fuel cells [3], oxygen sensors [4], adsorbents [5], thin films [6], thermal coatings and as luminescent material.

Pure ZrO_2 exist in three different polymorphs, monoclinic (m), tetragonal (t) and cubic (c), at room temperature and the fourth polymorph, orthorhombic (o), occurs only at high pressure.

Tetragonal ZrO_2 phase is the high temperature form of ZrO_2 and shows better properties than the room temperature form, m-ZrO_2. So, it is desirable to stabilize the t-ZrO_2 at room temperature. Additives are added to stabilize t-ZrO_2 to room temperature. In case of this work the phase is stabilized without the use of any additives but by controlling the growth of the particles.

Literature Review

V.I. Pârvulescu et al. [7] studied the preparation of mesoporous ZrO_2 by the method of polymeric sol-gel synthesis. Two different surfactants were used for the process of synthesis, $N(C_n)_4BR$ and $N(CH_3)_3C_nBr$ with variation of n from 8 to 18 and C_n being the linear alkyl chain. The obtained zirconium isopropoxide was hydrolyzed in three different ways including acid catalysis, base catalysis and acetylacetone as a stabilizer. The mesoporosity of these oxides can be controlled by modifying the n value and phase structure can controlled by changing the compositional parameters.

S. Wang et al. [8] used direct precipitation to prepare nano zirconia powder. They studied the variation in mean size, yield and dispersity of the prepared zirconia nano particles by varying five different parameters, molar ratio of $NH_3.H_2O$ to $ZrOCl_2$, C_2H_5OH percentage in reacting and washing solution, $ZrOCl_2$ concentration, precipitation temperature and surfactant PEG-800 dosage.

Blin et al. [9] synthesized nanostructured mesoporous ZrO_2 using $CTMABr-ZrOCl.8H_2O$. Their main aim was to optimize the synthesis condition without addition of any stabilizing agents like sulfate or phosphate ions. They reported the prepared material being of uniform pore size with a surface area of 300 $m^2 g^{-1}$. They also noticed a peculiar phenomenon, at low temperature or for short duration at high temperature, the prepared material showed the behavior of microporous but when the hydrothermal treatment is prolonged, the pores transformed to mesopores.

Rezaei et al. [10] prepared nanocrystalline, mesoporous and high surface ZrO_2 with tetragonal phase by surfactant-assisted route by using Pluronic P123 block copolymer as the surfactant. The surface area of the prepared powder was found to be 175 $m^2 g^{-1}$. The desired phase (tetragonal) and nano-structure was obtained after calcination at 600 °C for 5 hours. They utilized the Taguchi method of experimental design to optimize various parameters like molar ratio, pH of precipitation, aging time and zirconium molarity.

Miller et al. [11] studied the adsorption and desorption mechanism of nitrous oxide on zirconia. They used FTIR spectroscopy and mass spectroscopy as the tools to complete their study. They reported that Zr^{+4} ions are sites for molecular adsorption for N_2O and Zr^{+3} are sites for dissociative adsorption for N_2O at room temperature. Catalytic decomposition of N_2O occurs at temperature greater than 350 °C on ZrO_2 and follows first-order reaction kinetics. They also find

that there is no N-N bond dissociation during the process rather lattice oxygen atoms get incorporated into product oxygen molecules during the reaction.

Pokrovski et al. [12] studied the adsorption of CO and CO_2 on tetragonal and monoclinic phases of ZrO_2 using infrared spectroscopy and temperature-programmed desorption spectroscopy. They studied the adsorption process on t-ZrO_2 with surface areas of 20 and 187 m^2 g^{-1} and m-ZrO_2 with surface areas of 19 and 110 m^2 g^{-1}. They also reported the adsorption capacity of m-ZrO_2 higher than that of t-ZrO_2 for the case of CO_2 and CO because of higher strength of adsorption sites on this phase. The adsorbed species on m-ZrO_2 are HCO_3^- and m- and b-CO_3^{2-}, whereas for t-ZrO_2 are p- and b-CO_3^-.

Bachiller-Baeza et al. [13] studied the adsorption of CO_2 with the surface of different ZrO_2 polymorphs with the help of infrared spectroscopy, adsorption micro-calorimetry and temperature programmed desorption. They found that the crystallographic structure of ZrO_2 determines the number of different CO_2 adsorption sites on the surface of ZrO_2. m-ZrO_2 upon interaction with CO_2 forms HCO_3^-, m- and b-CO_3^{2-}, whereas b- and p-CO_3^{2-} were formed on the surface of t-ZrO_2. They also reported that m-ZrO_2 offers better adsorption sites for CO_2 than t-ZrO_2.

Nayak et al. [14] presented a novel way for the preparation of zirconia nanopowders via three different methods, gelation, precipitation and constant pH, through borohydride synthesis route. They reported the prepared ZrO_2 powders remained amorphous up to 600 °C and pure t-ZrO_2 remained stable up to 800 °C. Among the three methods, the constant pH route showed the highest activation energy of crystallization (E_a = 260 kJ/mol) or higher exothermic peak temperature at 717 °.

According to Garvie's Crystallite Size Theory [15], the stabilization of metastable tetragonal phase can be accounted to crystallite size effect. According to his theory, if the crystallite size is below a certain critical size, smaller than 30 nm, then tetragonal phase can be retained at temperatures below the transformation temperature.

Objectives
This research work focuses on the adsorption behavior of metal ions such as Fe, Ni and Co using zirconia nanopowders derived using borohydride route with and without CTAB.

Experimental

Synthesis Procedure

Pure t-ZrO$_2$ nanopowders were prepared by the method described by Nayak *et al.* [14] via borohydride synthesis route. The particle size reported by Nayak *et al.* [14] for precipitation route was ~30 nm. Two different types of ZrO$_2$ samples were prepared for the adsorption studies of metal ions – one with surfactant and the other without surfactant. The surfactant used in case was Cetyl Trimethyl Ammonium Bromide (CTAB). Both the samples were used for adsorption studies on Fe (III), Ni (II) and Co (II) metal ions separately for time periods of 15 minutes, 30 minutes, 60 minutes and 120 minutes.

For adsorption study of metal ions on our samples, three different solutions of metal ions Fe (III), Co (II) and Ni (II) of concentration 10 ppm, 1000 ppm and 1000 ppm were prepared by dissolving Ferric Chloride Hexahydrate (FeCl$_3$.6H$_2$O), Cobalt Chloride Hexahydrate (CoCl$_2$.6H$_2$O) and Nickel Chloride Hexahydrate (NiCl$_2$.6H$_2$O) in deionized water, respectively. The sorption studies were carried out in batch process in room temperature. 0.1 gm of adsorbent material was added to 20 ml of the metal ion solutions and contents were stirred with the help of a magnetic stirrer very slowly for 15 minutes, 30 minutes, 60 minutes and 120 minutes. The solutions was then filtered and the metal ions concentration were measured using UV-Vis spectroscopy. The metal ion removal efficiency was expressed in percentage and was calculated using the equation, $\frac{(c_i - c_f)}{c_i} \, x \, 100$ where C$_i$ and C$_f$ represent the initial and final concentration of metal ions concentration (mg L^{-1} or ppm) in solution. The mechanism of adsorption was studied by applying pseudo-first order and pseudo-second order equations to model the kinetics of the adsorption.

Characterization and Measurement

This section comprises of the various methods and techniques utilized for the detailed analysis of various properties of the synthesized material such as thermal properties, phase analysis, adsorption properties, crystallite size, pore size and distribution, microstructure analysis and surface area.

X-Ray Diffraction (XRD)

Phase analysis was studied using the X-ray diffraction (Rigaku, Japan) at room temperature with filtered 0.154056 nm Cu-Kα radiation. Samples were scanned in a continuous mode from 200-800 at a scanning rate of 200/min.

Brunauer, Emmett and Teller (BET) Measurements

The specific surface area of a powder was determined using BET. Particle size was also determined from surface area using the following equation.

$$D_{BET} = \frac{6000}{\rho S_w}$$

Where D_{BET} is the particle size of sample, ρ is the density of the sample and S_w is the surface area obtained from BET measurements. The density of t-ZrO_2 is 5.68 g cc^{-1}.

Field Emission Scanning Electron Microscopy (FESEM)

Microstructural features were studied using Felid Emission Scanning Electron Microscope (NOVA, NanoSEM). One pinch of the well-grinded sample powder was deposited on to the carbon tape pasted on the brass plate. This brass plate was coated for 5 minutes and then used for microscopy.

Ultraviolet-Visible Spectroscopy (UV-Vis)

The concentration of absorbing species in a solution was analyzed using Ultraviolet-Visible spectrum.

Results and Discussion
X-Ray Diffraction (XRD)

The as-prepared samples were subjected to a calcining environment of 600 °C for 1 hour after which they are analyzed by X-ray diffractograms for confirming the phase and to determine the crystallite size. Pattern indicates that the formed sample is crystalline in nature. X-ray diffractograms confirmed the formation of t-ZrO_2 phase. Crystallite size of the sample was determined with the help of Scherrer formula and was found to be 7.3 nm.
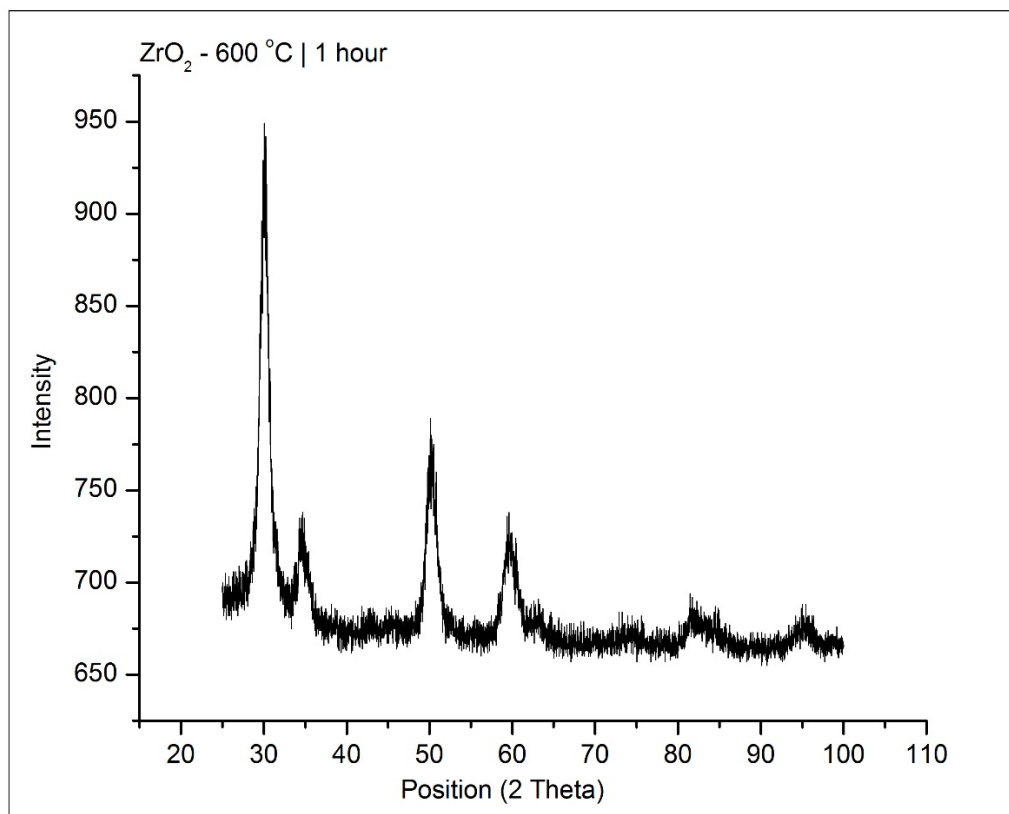

Figure 1: XRD pattern of calcined sample at 600 °C for 1 hour

Brunauer, Emmett and Teller (BET) Measurements

From BET instrument, it was determined that the surface area of the samples after calcination at 600 °C for 1 hour was 55 m^2 g^{-1}. The particle size of the samples was found to be 19.2 nm.

UV-Vis Spectroscopy

With the help of UV-Vis spectroscopy, removal efficiency of the adsorbate material was determined using Beer-Lambert Law.

Fig. 2, 3 and 4 show the adsorption behavior of Co, Ni and Fe using ZrO_2 powders prepared without addition of CTAB. The calcined samples without surfactant showed the removal efficiency of 13.86 % for Co (II) with a concentration of 1000 ppm at 15 minutes. The value increased to 18.81 % with an adsorption time of 120 minutes.

In addition, removal efficiency for Ni (II) with a concentration of 1000 ppm was very less by the calcined samples without surfactant. At 15 minutes, the removal efficiency was found to be 4.66 % and it increased to 7.33 % at 120 minutes.
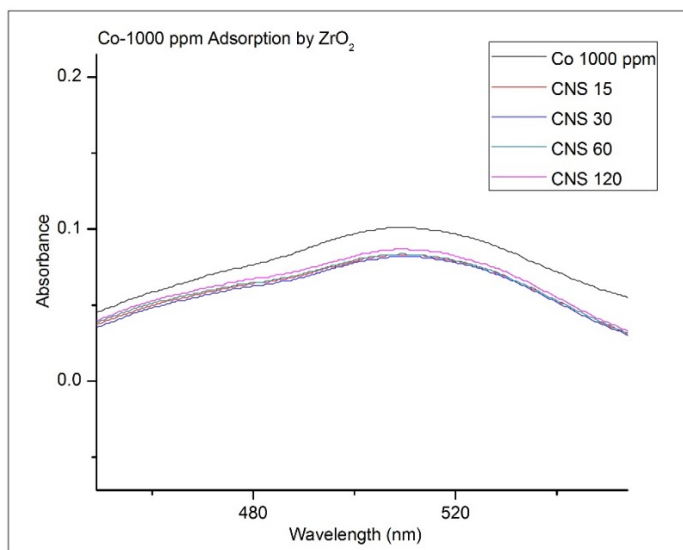
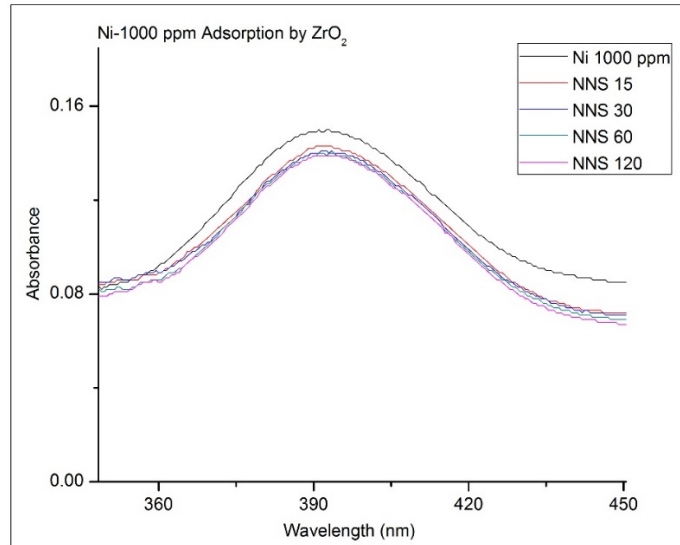**Figure 2: Adsorption of Co (II) 1000 ppm by ZrO_2**

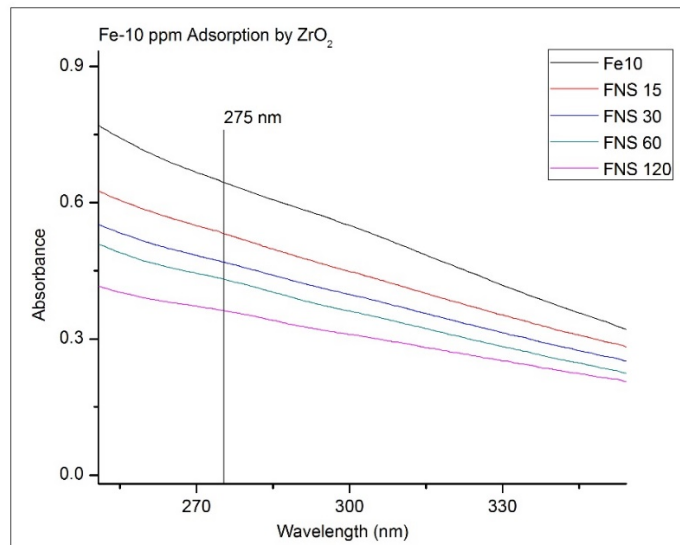**Figure 3: Adsorption of Ni (II) 1000 ppm by ZrO$_2$**

Figure 4: Adsorption of Fe (III) 10 ppm by ZrO$_2$

The removal efficiency was found to be 17.49 % at 15 minutes whereas it increased to a value of 43.81 % at 120 minutes. Since, the removal efficiency for Fe (III) was satisfactory as confirmed from Fig. 4, it was further investigated for the type of adsorption (see Figure 5) and order of reaction (see Figure 6) it was following during the reaction.
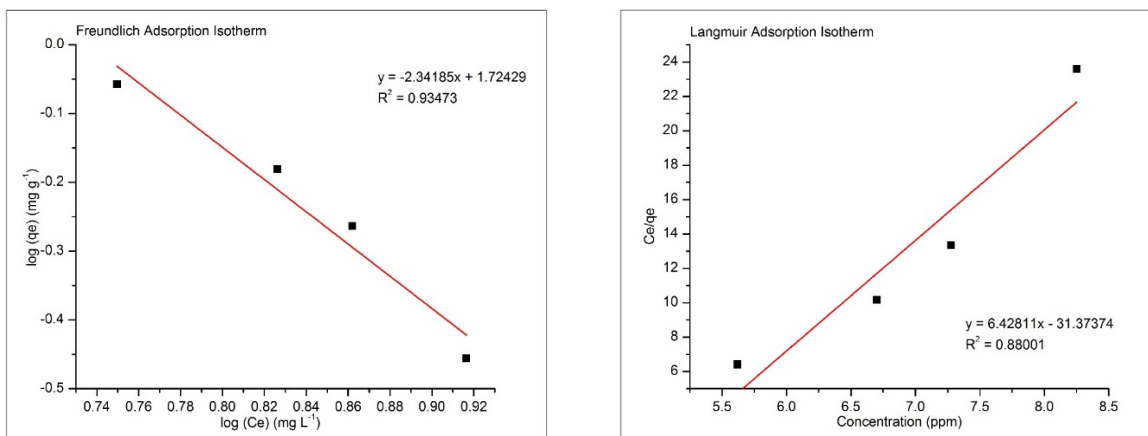
Figure 5: (a) Freundlich and (b) Langmuir Adsorption Isotherm of ZrO₂ for Fe-10 ppm

When the derived data were fitted to the Freundlich adsorption isotherm, it showed a R^2 value of 0.935. The adsorption intensity and adsorption capacity was found to be -2.342 and 53.002 mg g^{-1} respectively.

When the derived data points were fitted into Langmuir adsorption isotherm, it showed a R^2 value of 0.88 with q_m value and K_L being equal to 0.032 mg g^{-1} and 4.881 L mg^{-1} respectively. The R_L value calculated from K_L value was found to be 0.020 which is $0 < R_L < 1$. Hence, the shape of the isotherm is favorable.

Since the R^2 value of Freundlich was higher than that of Langmuir, the adsorption sites were confirmed to be non-uniform in nature and having heterogeneous surface.
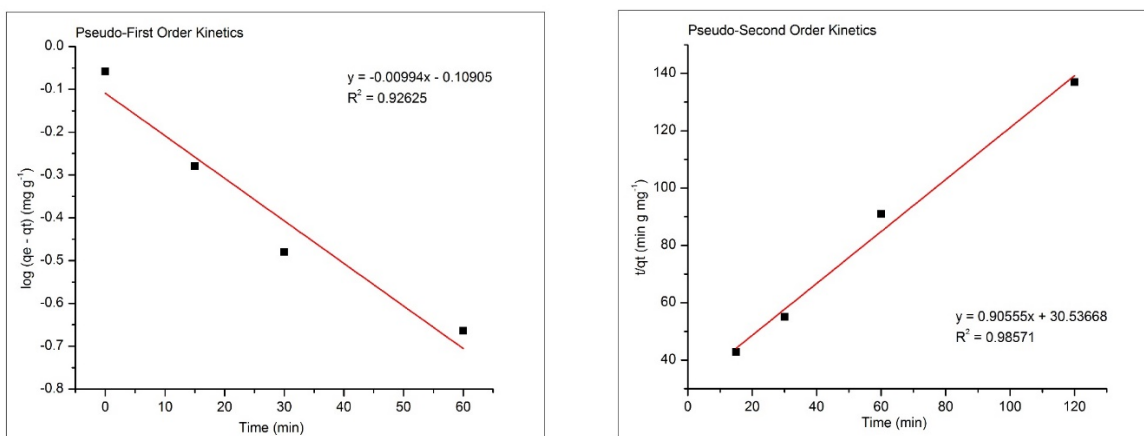

Figure 6: (a) Pseudo-First and (b) Pseudo-Second Order Kinetics of ZrO₂ for Fe-10 ppm

The R^2 value for the pseudo-first order was found to be 0.926. The rate constant and q_e of the equation was found to be -0.0229 min^{-1} and 0.778 mg g^{-1}.

The R^2 value for the case of pseudo-second order kinetics was found to be 0.986. The q_e and the rate of the reaction was found to be 1.104 mg g^{-1} and 0.027 g mg^{-1} min^{-1}. By comparing the R^2 value it is clear the reaction followed the pseudo-second order kinetics.

Figure 7 shows a comparison between the removal efficiency of ZrO_2 for the three different metal ions. From the figure, it is clear that Fe (III) with 10 ppm concentration showed the maximum efficiency whereas Ni (II) with 1000 ppm concentration showed the minimum efficiency. From of the slope of the curves at different position, it was identified that the initial rate of the adsorption was high and it decreased after 60 minutes of adsorption time. Since, less number of adsorption sites were available after 60 minutes, the rate of adsorption was decreased.
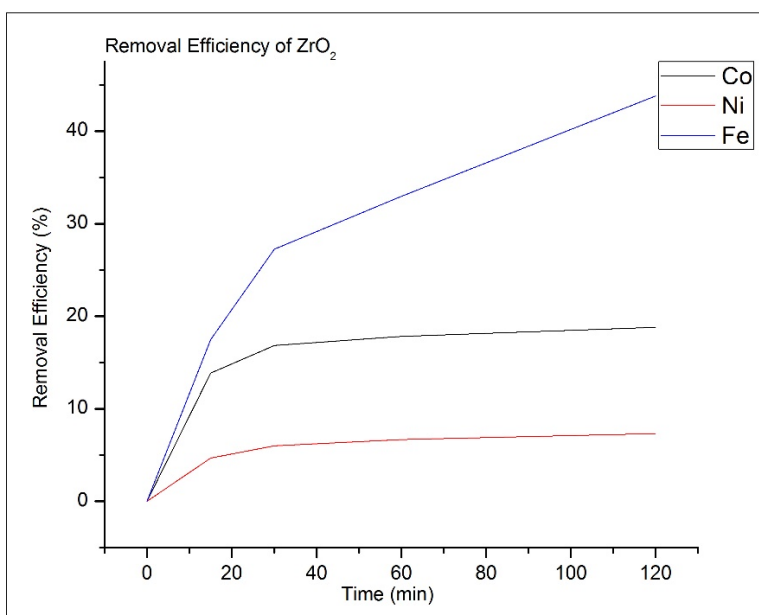

Figure 7: Removal Efficiency of ZrO_2

Figure 8 shows the absorbance behavior for Co (II) 1000 ppm being adsorbed on ZrO_2+CTAB sample. For this case, removal efficiency of 24.75 % was observed after 15 minutes and it increased to value of 34.65 % after 120 minutes.
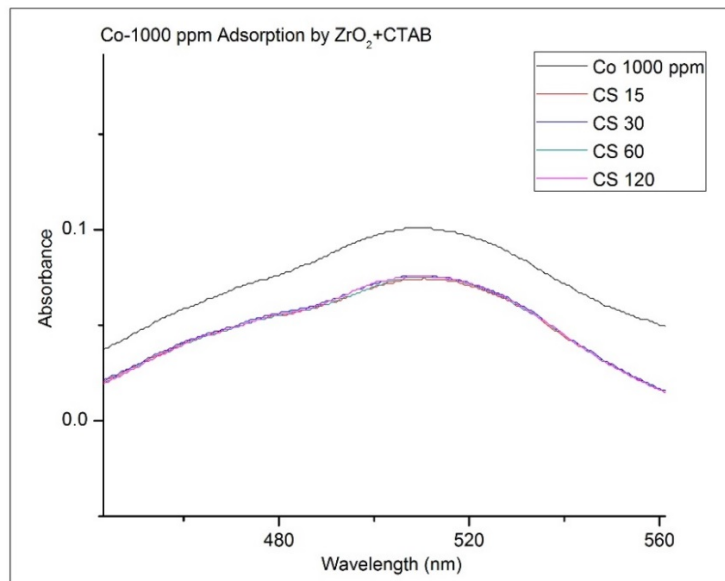
Figure 8: Adsorption of Co (II) 1000 ppm by ZrO₂+CTAB

Figure 9 shows the adsorption of Ni (II) with a concentration of 1000 ppm by ZrO_2+CTAB. The calcined samples showed good adsorption for this case. A removal efficiency of 23.33 % was achieved after 15 minutes and reached to value of 51 % after 120 minutes.
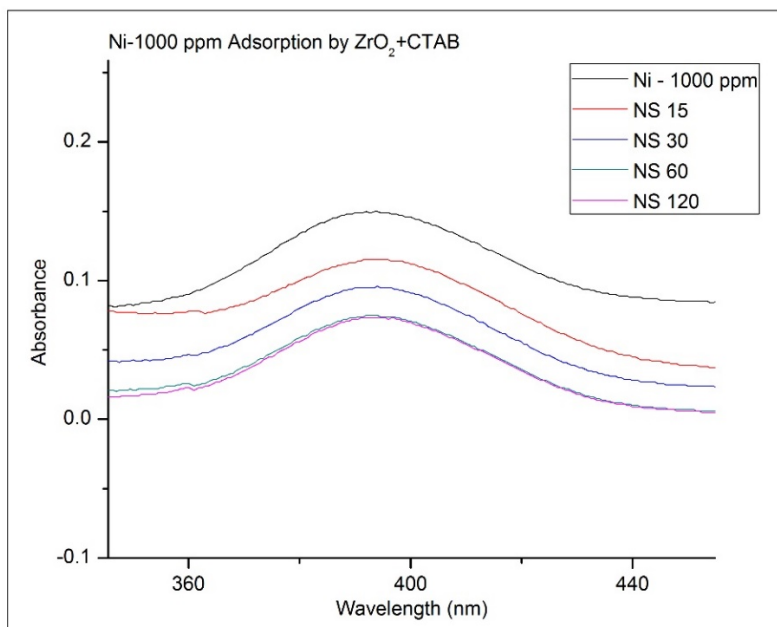

Figure 9: Adsorption of Ni (II) 1000 ppm by ZrO₂+CTAB

Figure 10 shows adsorption phenonmenon of ZrO_2+CTAB for Fe (III) with concentration of 10 ppm. Calcined samples showed exceptional resutls for this case. A removal efficiency of 77.08 % was achieved only after 15 minutes and it further increased toa value of 84.52 % after 120 minutes.
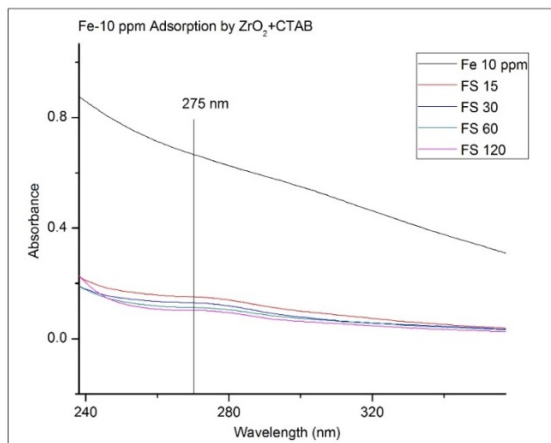

Figure 10: Adsorption of Fe (III) 10 ppm by ZrO_2+CTAB

Figure 11 shows a clear comparison between the removal efficiency of ZrO_2+CTAB for the three different metal ions. Fe (III) case showed the highest removal efficiency whereas Co (II) showed the lowest removal efficiency.
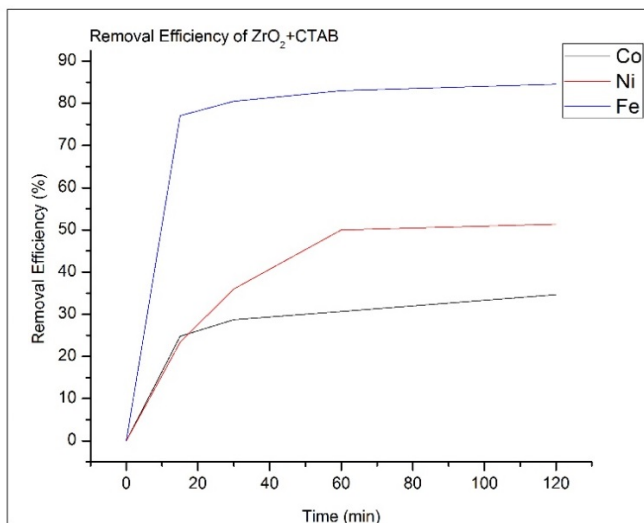

Figure 11: Removal Efficiency of ZrO_2+CTAB

Since Ni (II) and Fe (III) showed satisfactory adsorption phenomenon, these two were further investigated for the adsorption isotherm (Figure 12) and type of reaction kinetics (Figure 13) these were following.
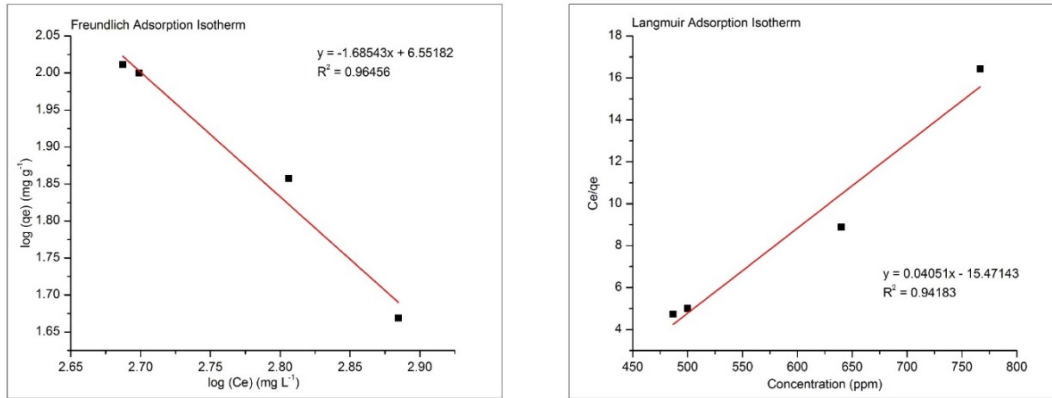

Figure 12: (a) Freundlich and (b) Langmuir Adsorption Isotherm of ZrO_2+CTAB for Ni-1000 ppm

For Freundlich adsorption isotherm, the R^2 was found to be 0.965 with adsorption intensity and adsorption capacity being -1.685 and 3563034.274 respectively.

The R^2 value for Langmuir adsorption isotherm was found to be 0.942 with q_m and K_L being equal to 0.065 mg g^{-1} and 381.916 respectively. From K_L, R_L was calculated which showed a value of 0.0000026. If we consider this value to be 0, then the reaction is irreversible in nature but if the value is not considered to be 0, then it shows a favorable shape of isotherm. By comparing the R^2 value of both isotherm, it is clear that the phenomenon is following Freundlich adsorption isotherm.
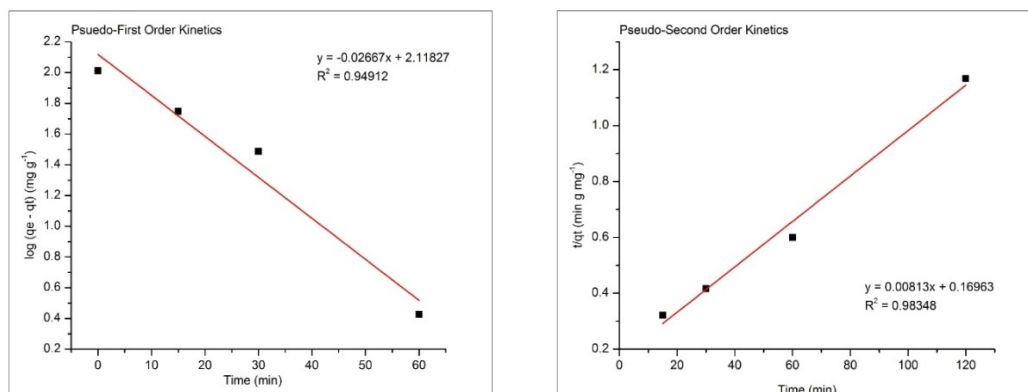

Figure 13: (a) Pseudo-First and (b) Pseudo-Second Order Kinetics of ZrO_2+CTAB for Ni-1000 ppm

The R^2 value for pseudo-first order kinetics was found to be 0.949 with rate constant and q_e being equal to -0.061 and 131.302 mg g^{-1}.

The R^2 value for pseudo-second order kinetics was found to be 0.983 with q_e and rate constant values being found to be equal to 123.001 mg g^{-1} and 0.00038 g mg^{-1} min^{-1} respectively. By comparing the R^2, we can conclude that the reaction was pseudo-second order in nature.

Since, ZrO$_2$ with CTAB showed desirable result for Fe (III) case, it was further investigated for the adsorption phenonmena and kinetics of the reaction. Obtained data was fitted for both Langmuir adsorption isotherm as well as Freundlich adsorption isotherm (Figure 14). Langmuir adsorption isotherm showed a R^2 value of 0.972 whereas Freundlich adsorption isotherm showed a R^2 value of 0.993. From the R^2 value, it was clear that the reaction followed Freundlich adsorption phenomenon. From the Langmuir adsorption isotherm, the monolayer adsorption capacity (q_m) was determiend to be 1.316 mg g^{-1} and separation constant (R_L) value was found to be 0.0256, which is 0 < R_L < 1 and hence a favorable shape of the isotherm was obtained. From the Freundlich adsorption isotherm, adsorption intensity (1/n) was determined to be − 0.235 and adsorption capacity (K_F) was found to be 1.875.
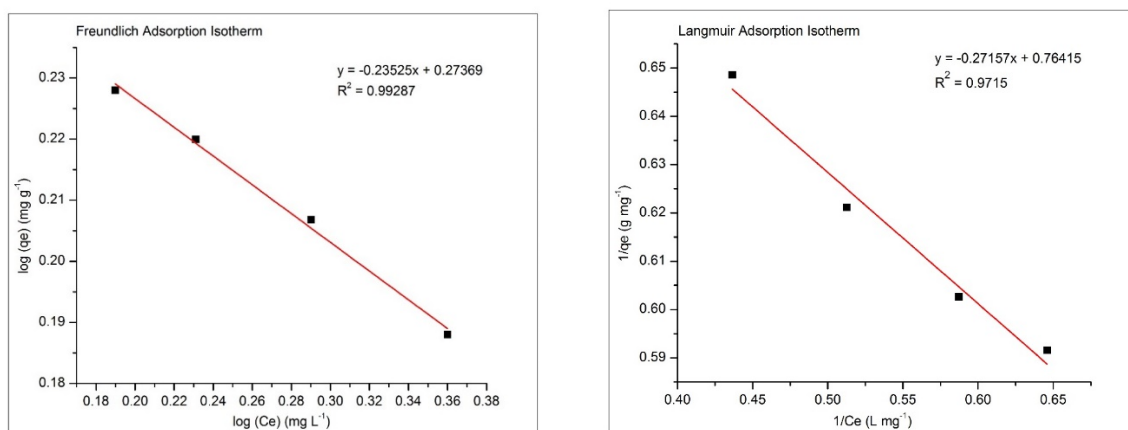

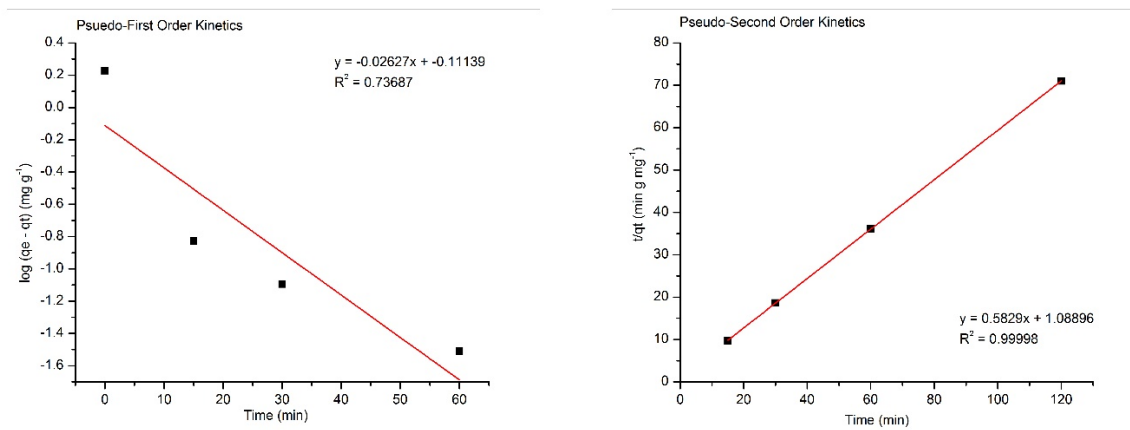**Figure 14: (a) Freundlich and (b) Langmuir adsorption isotherm for Fe (III) adsorption by ZrO$_2$+CTAB**

Figure 15: (a) Pseudo-First and (b) Pseudo-Second Order Kinetics of ZrO_2+CTAB for Fe-10 ppm

The obtained data were also used to determine the kinetics of the reaction (Figure 15). Derived data were again fitted for psuedo-first order and pseudo-second order reaction. Pseudo-first order reaction provided a R^2 value of 0.73 whereas for pseudo-second order reaction the R^2 value was found to be 0.99. So, the reaction followed a pseudo-second order kinetics. From the pseudo-first order reaction, the rate constant (K_1) was found to be -0.0481 min^{-1} and the amount of Fe (III) adsorbed at the time of equilibrium (q_e) was found to be 0.776 mg g^{-1}. The rate constant for pseudo-second order reaction was found to be 0.331 g mg^{-1} min^{-1} and the amount of Fe (III) adsorbed at the time of equilibrium (q_e) was found to be 1.718 mg g^{-1}.

FESEM

After completion of the corresponding adsorption time, the solution was filtered. The filtered paper used in the process of filtering was dried at 80 °C for 24 hours after completion of filtering. Residue powder was collected and grinded for the FESEM micrographs and elemental mapping.

Figure 16 (b), 17 (b) and 18 (b) provides a clear evidence that the amount of presence of Fe has increased after the corresponding time intervals. Elemental mapping also confirms the amount of adsorption has increased with the passage of time.
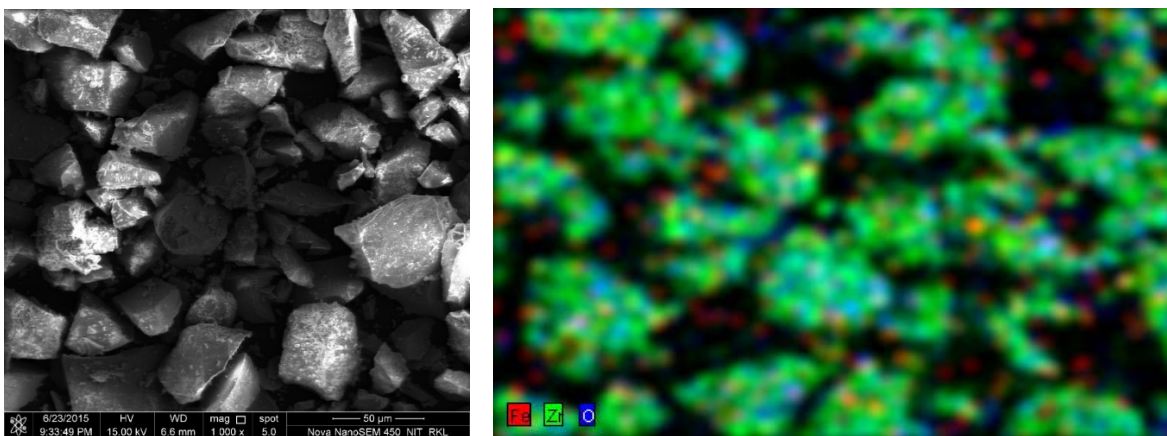
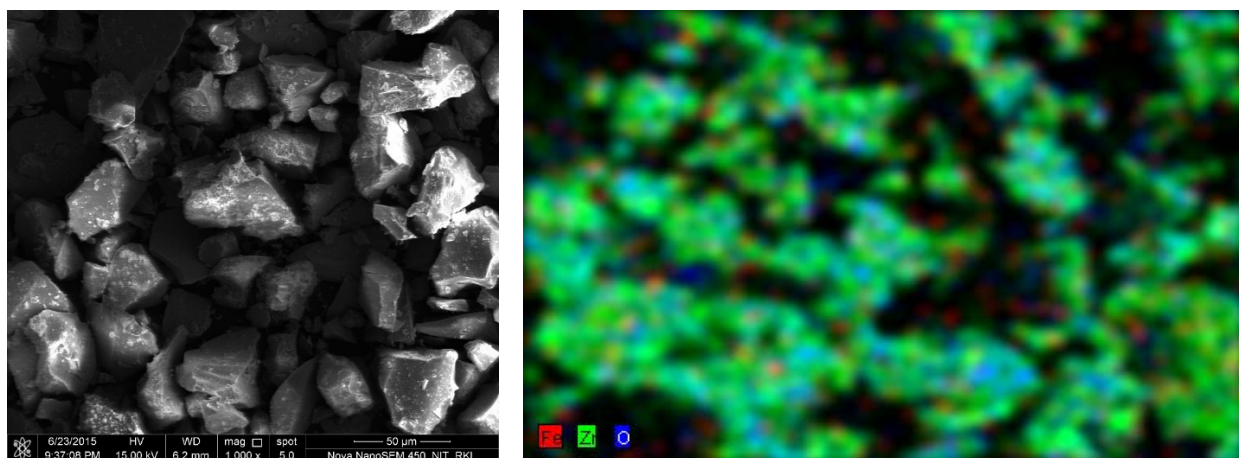**Figure 16: (a) FESEM image and (b) Elemental mapping of Fe (III) adsorbed ZrO$_2$+CTAB after 15 minutes**

Figure 17: (a) FESEM image and (b) Elemental mapping of Fe (III) adsorbed ZrO$_2$+CTAB after 60 minutes
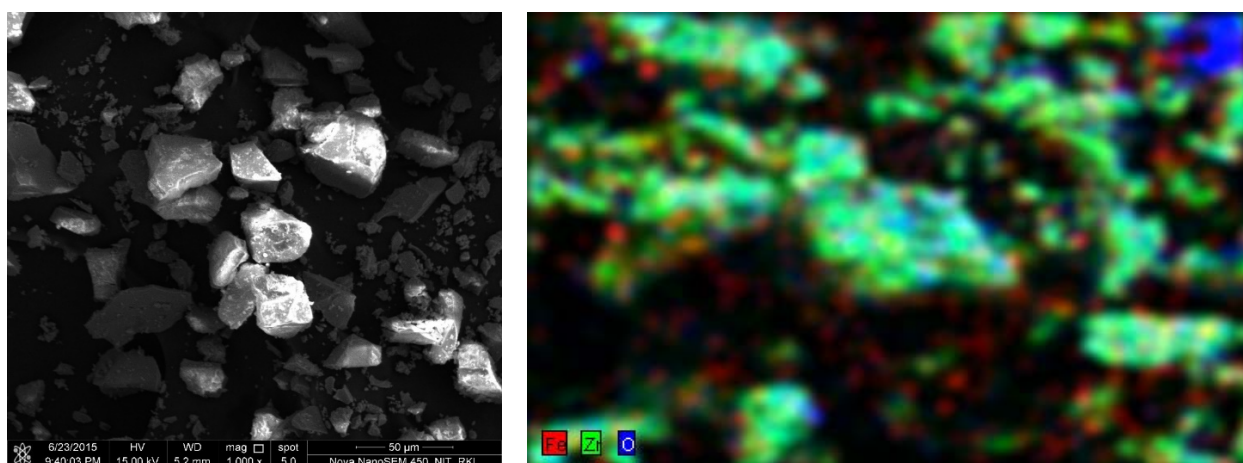

Figure 18: (a) FESEM image and (b) Elemental mapping of Fe (III) adsorbed ZrO$_2$+CTAB after 120 minutes

Figure 19 (b) shows the elemental mapping of Co, Zr and O after 120 minutes of adsorption by ZrO_2+CTAB. The figure clearly shows the adsorbed Co over the surface of ZrO_2.
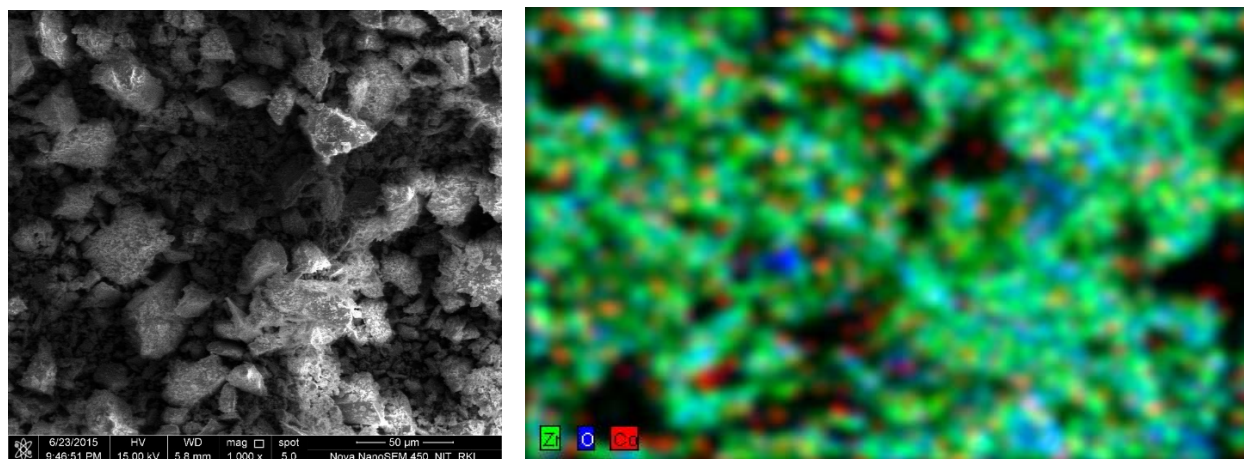

Figure 19: (a) FESEM image and (b) Elemental mapping of Co (II) adsorbed ZrO_2+CTAB after 120 minutes

Figure 20 (b) shows the elemental mapping of Ni, Zr and O after 120 minutes of adsorption by ZrO_2+CTAB. The figure clearly shows the adsorption sites of Ni over the ZrO_2 samples.
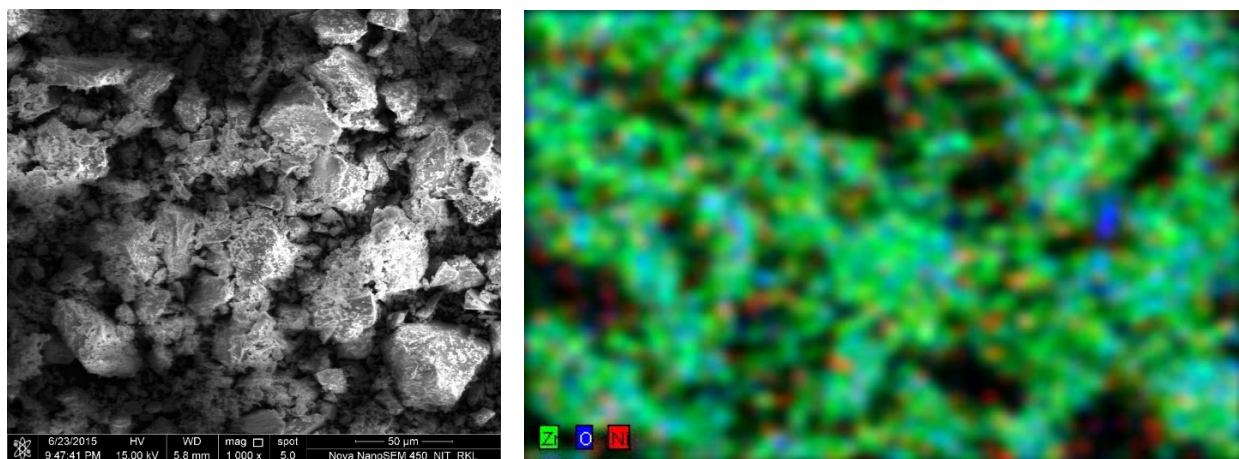

Figure 20: (a) FESEM image and (b) Elemental mapping of Ni (II) adsorbed ZrO_2+CTAB after 120 minutes

Conclusions

Two different types of ZrO_2 samples were prepared by precipitation route via borohydride method. One sample was ZrO_2 prepared without surfactant while the other was prepared by the same route but with the addition of CTAB surfactant. Prepared samples were characterized using XRD which confirmed the phase as t-ZrO_2 with a crystallite size of 7.3 nm. BET measurements provided a surface area of 55 m^2 g^{-1} with a particle size of 19.2 nm. Adsorption studies of both the prepared samples were carried out on three different metal ion, Fe (III), Co (II) and Ni (II). Adsorption studies confirmed the adsorption isotherm being Freundlich adsorption isotherm which is a clear indication about the heterogeneous surface and non-uniform adsorption. From the obtained data, it was determined that the reaction followed a pseudo-second order kinetics. In case of without surfactant, Fe case showed the highest adsorption with a removal efficiency value of 43.81 % after 120 minutes whereas Ni case showed the least adsorption with a removal efficiency value of 7.33 % after 120 minutes. Co case showed the removal efficiency of 18.81 % after 120 minutes. For the case of CTAB, Fe case showed a removal efficiency of 84.52 %, Co case showed a removal efficiency of 34.65 % and Ni case showed a removal efficiency of 51.33 %. From these data, it was also concluded that ZrO_2+CTAB shows better adsorption than pure ZrO_2 samples.

Reference

1. R. C. Garvie, R. H. Hannink and R. T. Pascoe, "Ceramic Steel?", Nature, 258, 703-704 (1975).

2. C. Bernard, B. Laurence and V. Franceline, US patent 20020031675.

3. F. Tietz, H.-P. Buchkremer and D. Stover, Solid State Ionics, 152–153 (2002) 373-381.

4. S.A. Ghom, C. Zamani, S. Nazarpour, T. Andreu, and J.R. Morante, Sensors and Actuators B, 140(2009) 216-221.

5. I. Nukatsuka and H. Yamane, Adsorpt. Sci. Technol., 29 (2011), 1025-1033.

6. Y.-S. Ko and Y.-U. Kwon, ACS Appl. Mater. Interfaces, 5 (2013) 3599-3606.

7. V.I. Pârvulescu, H. Bonnemann, V. Pârvulescu, U. Endruschat, A. Rufinska, Ch. W. Lehmann, B. Tesche and G. Poncelet, "Preparation and characterisation of mesoporous zirconium oxide", Applied Catalysis A: General, 214, 273–287 (2001).

8. Shaoyan Wang, Xiaoan Li, Yuchun Zhai and Kaiming Wang, "Preparation of homodispersed nano zirconia", Powder Technology, 168, 53–58 (2006).

9. J.L. Blin, R. Flamant and B.L. Su, "Synthesis of nanostructured mesoporous zirconia using CTMABr–ZrOCl.8H2O systems: a kinetic study of synthesis mechanism", International Journal of Inorganic Materials, 3, 959–972 (2001).

10. M. Rezaei, S.M. Alavi, S. Sahebdelfar and Zi-Feng Yan, "Tetragonal nanocrystalline zirconia powder with high surface area and mesoporous structure", Powder Technology, 168, 59–63 (2006).

11. T. M. Miller and V. H. Grassian, "A mechanistic study of nitrous oxide adsorption and decomposition on zirconia", Catalysis Letters, 46, 213-221 (1997).

12. Konstantin Pokrovski, Kyeong Taek Jung and Alexis T. Bell, "Investigation of CO and CO2 Adsorption on Tetragonal and Monoclinic Zirconia", Langmuir, 17, 4297-4303 (2001).

13. B. Bachiller-Baeza, I. Rodriguez-Ramos and A. Guerrero-Ruiz, "Interaction of Carbon Dioxide with the Surface of Zirconia Polymorphs", Langmuir, 14, 3556-3564 (1998).

14. N. B. Nayak, B. B. Nayak and A. Mondal, "Enhanced Activation Energy of Crystallization of Pure Zirconia Nanopowders Prepared via an Efficient Way of Synthesis Using NaBH4", J. Am. Ceram. Soc., 96 [11] 3366-3368 (2013).

15. R.C. Garvie, J. Phys. Chem., 69 (1965) 1238-1243.